

Flavor SU(3) analysis of charmless B meson decays to two pseudoscalar mesons

Cheng-Wei Chiang

*Department of Physics, National Central University, Chungli, Taiwan 320,
R.O.C. and
Institute of Physics, Academia Sinica, Taipei, Taiwan 115, R.O.C.
E-mail: chengwei@phy.ncu.edu.tw*

Yu-Feng Zhou

*Theory Group, KEK, Tsukuba, 305-0801, Japan.
E-mail: zhou@post.kek.jp*

ABSTRACT: Global fits to charmless $B \rightarrow PP$ decays in the framework of flavor SU(3) symmetry are updated and improved without reference to the $\sin 2\beta$ measured from the charmonium decay modes. Fit results directly constrain the $(\bar{\rho}, \bar{\eta})$ vertex of the unitarity triangle, and are used to predict the branching ratios and CP asymmetries of all decay modes, including those of the B_s system. Different schemes of SU(3) breaking in decay amplitude sizes are analyzed. The major breaking effect between strangeness-conserving and strangeness-changing decays can be accounted for by including a ratio of decay constants in tree and color-suppressed amplitudes. The possibility of having a new physics contribution to $K\pi$ decays is also examined from the data fitting point of view.

KEYWORDS: B Mesons, Weak Decays, Unitarity Triangle.

Contents

1. Introduction	1
2. Formalism and Notation	2
3. Fitting Analysis	6
3.1 Fits to modes with only π, K mesons in the final state	7
3.2 Fits to all $B \rightarrow PP$ modes	13
3.3 Fits with a new physics amplitude	15
4. Summary	16

1. Introduction

In the standard model (SM) of particle physics, CP violation in the quark sector is postulated to be purely derived from the Kobayashi-Maskawa mechanism, in which a 3×3 unitary CKM matrix V_{CKM} with three mixing angles and one CP-violating phase is used to describe charge-current weak transitions between the up-type and down-type quarks [1]. The unitarity condition on the first and third columns of the CKM matrix is often used to form a triangle on the complex plane because the lengths of its three sides are of the same order. An important program in flavor physics is to constrain this unitarity triangle using as many independent experimental inputs as possible, for both determining standard model (SM) parameters with high precisions and discovering any possible new physics effect. A lot of progress has been done in this direction with the help of a huge amount of B meson data collected in the past few years at the B -factories [2, 3].

Although charmless modes are rare processes in B decays, they are very sensitive to the smallest CKM matrix elements V_{ub} and V_{td} through decay amplitudes and mixing, respectively. Moreover, they provide us information about the weak phases associated with these two matrix elements. Some theoretical analyses have been done in recent years to globally fit to charmless $B \rightarrow PP$ and VP decay data in the framework of QCD factorization [4] and flavor SU(3) symmetry [5, 6, 7, 8]. Here P and V refer to pseudoscalar and vector mesons, respectively. Since the weak phase β (ϕ_1) is more accurately determined from the time-dependent CP asymmetry analysis of $B_d \rightarrow (\bar{c}c)K_S$ modes, the result is usually used as an input in the theory

parameters. With more modes being observed and measured at higher precisions, it becomes possible to use purely rare decays to provide a completely independent determination of the unitarity triangle vertex $(\bar{\rho}, \bar{\eta})$, expressed in terms of the Wolfenstein parameters [9], without reference to the charmonium modes. It is therefore one objective of the current analysis to see whether the charmless B decay data alone also provide a CKM picture consistent with other constraints.

In this paper, we perform χ^2 fits to the available charmless $B \rightarrow PP$ decays using the flavor diagram approach [10]. The fitting parameters include the Wolfenstein parameters A , $\bar{\rho}$, and $\bar{\eta}$, magnitudes of different flavor amplitudes, and their associated strong phases. To take into account SU(3) breaking, we also include breaking factors of amplitude sizes as our fitting parameters in some fits. Generally speaking, our fits render an area of the $(\bar{\rho}, \bar{\eta})$ vertex slightly deviated from but still consistent with that obtained from other constraints. Aside from a decay constant ratio, the SU(3) breaking is seen at $O(10)\%$ level. From the extracted ranges of theory parameters, we predict the branching ratios and CP asymmetries of all decays using flavor SU(3) symmetry, including the B_s system. The latter will be compared with data already or to be measured at the Tevatron, large hadron collider (LHC), and KEKB upgraded for running at $\Upsilon(5S)$.

This paper is organized as follows. In Section 2, we introduce the notations used in this analysis, including the fitting parameters. Flavor amplitude decompositions of the rare decay modes, along with the available experimental data on branching ratios and CP asymmetries, are summarized in this section. The fitting schemes and results are presented in Section 3, where predictions and outlook of yet-seen modes are also given. Finally, Section 4 summarizes our findings.

2. Formalism and Notation

The magnitude of invariant decay amplitude \mathcal{A} for a decay process $B \rightarrow M_1 M_2$ is related to its partial width via the following relation:

$$\Gamma(B \rightarrow M_1 M_2) = \frac{|\mathbf{p}|}{8\pi m_B^2} |\mathcal{A}|^2, \quad (2.1)$$

where \mathbf{p} is the 3-momentum of the final state particles in the rest frame of the B meson. To relate partial widths to branching ratios, we use the world-average lifetimes $\tau^+ = (1.638 \pm 0.011)$ ps, $\tau^0 = (1.530 \pm 0.009)$ ps and $\tau_{B_s} = (1.466 \pm 0.059)$ ps computed by the Heavy Flavor Averaging Group (HFAG) [14]. Unless otherwise indicated, for each branching ratio quoted we imply the average of a process and its CP -conjugate one.

To perform the flavor amplitude decomposition, we use the following quark content and phase conventions for mesons:

- *Bottom mesons:* $B^0 = d\bar{b}$, $\bar{B}^0 = b\bar{d}$, $B^+ = u\bar{b}$, $B^- = -b\bar{u}$, $B_s = s\bar{b}$, $\bar{B}_s = b\bar{s}$;

- *Pseudoscalar mesons*: $\pi^+ = u\bar{d}$, $\pi^0 = (d\bar{d} - u\bar{u})/\sqrt{2}$, $\pi^- = -d\bar{u}$, $K^+ = u\bar{s}$, $K^0 = d\bar{s}$, $\bar{K}^0 = s\bar{d}$, $K^- = -s\bar{u}$, $\eta = (s\bar{s} - u\bar{u} - d\bar{d})/\sqrt{3}$, $\eta' = (u\bar{u} + d\bar{d} + 2s\bar{s})/\sqrt{6}$;

The η and η' mesons correspond to octet-singlet mixtures

$$\eta = \eta_8 \cos \theta_0 - \eta_1 \sin \theta_0 , \quad (2.2)$$

$$\eta' = \eta_8 \sin \theta_0 + \eta_1 \cos \theta_0 . \quad (2.3)$$

As shown in Ref. [5], varying the mixing angle θ_0 does not improve the quality of fits. Therefore, here we fix $\theta_0 = \sin^{-1}(1/3) \simeq 19.5^\circ$ according to the above-mentioned quark contents of η and η' .

We list flavor amplitude decompositions and averaged experimental data for $B \rightarrow PP$ decays in Tables 1 and 2. Values of measured observables are obtained by weighted-averaging over the results of the BaBar [15, 16, 17, 18, 19, 20, 21, 22, 23], Belle [24, 25, 26, 27, 28, 29], CLEO [30, 31, 32, 33, 34], and CDF [35, 36, 37] Collaborations. The standard deviation is scaled by the scale factor S (whose definition can be found, for example, in Ref. [11]) if it is greater than 1 in order to take into account the discrepancy among different experimental groups. These include: $Br(\pi^-\pi^0)$ ($S = 1.3$), $Br(\pi^-\eta)$ ($S = 1.1$), $Br(\pi^-\eta')$ ($S = 1.4$), $\mathcal{A}(\pi^+\pi^-)$ ($S = 2.6$), $Br(\pi^0\eta')$ ($S = 1.4$), $A_{CP}(K^-\pi^0)$ ($S = 1.3$), $Br(K^-\eta)$ ($S = 1.3$), $Br(\eta'\bar{K}^0)$ ($S = 1.3$), and $\mathcal{A}(\eta'K_S)$ ($S = 1.4$). Amplitudes such as annihilation and exchange diagrams are expected to be small and therefore neglected in the calculation.

In the present approximation, we consider five dominant types of independent amplitudes: a ‘‘tree’’ contribution T ; a ‘‘color-suppressed’’ contribution C ; a ‘‘QCD penguin’’ contribution P ; a ‘‘flavor-singlet’’ contribution S , and an ‘‘electroweak (EW) penguin’’ contribution P_{EW} . The former four types are considered as the leading-order amplitudes, while the last one is higher order in weak interactions. There are also other types of amplitudes, such as the ‘‘color-suppressed EW penguin’’ diagram P_{EW}^C , ‘‘exchange’’ diagram E , ‘‘annihilation’’ diagram A , and ‘‘penguin annihilation’’ diagram PA . Due to dynamical suppressions, these amplitudes are ignored in the analysis. This agrees with the recent observation of the $B^0 \rightarrow K^+K^-$ decay.

The QCD penguin amplitude in fact contains three components (apart from the CKM factors): P_t , P_c , and P_u , with the subscript denoting which quark is running in the loop. After imposing the unitarity condition, we are left with two components: $P_{tc} = P_t - P_c$ and $P_{tu} = P_t - P_u$, integrating out the t quark from the theory. For simplicity, we will assume the t -penguin dominance, so that $P_{tc} = P_{tu}$ and are denoted by a single symbol P . The same comment applies to other penguin-type amplitudes (e.g., P_{EW} and P_{EW}^C) as well.

In physical processes, the above-mentioned flavor amplitudes always appear in specific combinations. To simplify the notations, we therefore define the following unprimed and primed symbols for $\Delta S = 0$ and $|\Delta S| = 1$ transitions, respectively:

$$t \equiv Y_{db}^u T - (Y_{db}^u + Y_{db}^c) P_{EW}^C , \quad t' \equiv Y_{sb}^u \xi_t T - (Y_{sb}^u + Y_{sb}^c) P_{EW}^C ,$$

Mode	Flavor Amplitude	BR	\mathcal{A}_{CP}		
$B^- \rightarrow$	$\pi^- \pi^0$	$-\frac{1}{\sqrt{2}}(t+c)$	5.7 ± 0.5	0.04 ± 0.05	
	$K^- \bar{K}^0$	p	1.4 ± 0.3	0.12 ± 0.18	
	$\pi^- \eta$	$-\frac{1}{\sqrt{3}}(t+c+2p+s)$	4.4 ± 0.4	-0.19 ± 0.07	
	$\pi^- \eta'$	$\frac{1}{\sqrt{6}}(t+c+2p+4s)$	2.6 ± 0.8	0.15 ± 0.15	
$\bar{B}^0 \rightarrow$	$K^+ K^-$	$-(e+pa)$	0.07 ± 0.11	-	
	$K^0 \bar{K}^0$	p	1.0 ± 0.2	-	
	$\pi^+ \pi^-$	$-(t+p)$	5.2 ± 0.2	0.39 ± 0.19 -0.58 ± 0.09	
	$\pi^0 \pi^0$	$\frac{1}{\sqrt{2}}(-c+p)$	1.3 ± 0.2	0.36 ± 0.32	
	$\pi^0 \eta$	$-\frac{1}{\sqrt{6}}(2p+s)$	0.60 ± 0.46	-	
	$\pi^0 \eta'$	$\frac{1}{\sqrt{3}}(p+2s)$	1.2 ± 0.7	-	
	$\eta \eta$	$\frac{1}{3\sqrt{2}}(2c+2p+2s)$	< 1.2	-	
	$\eta \eta'$	$-\frac{1}{3\sqrt{2}}(2c+2p+5s)$	< 1.7	-	
	$\eta' \eta'$	$\frac{1}{3\sqrt{2}}(c+p+4s)$	< 10	-	
	$\bar{B}_s^0 \rightarrow$	$K^+ \pi^-$	$-(t+p)$	< 5.6	-
		$K^0 \pi^0$	$-\frac{1}{\sqrt{2}}(-c+p)$	-	-
		$\bar{K}^0 \eta$	$-\frac{1}{\sqrt{3}}(c+s)$	-	-
		$\bar{K}^0 \eta'$	$\frac{1}{\sqrt{6}}(c+3p+4s)$	-	-

Table 1: Flavor amplitude decompositions for strangeness-conserving $B \rightarrow PP$ decays. Measured branching ratios (in units of 10^{-6}) and CP asymmetries are given in the last two columns. For those modes with time-dependent CP asymmetries, \mathcal{A} and \mathcal{S} are listed in the first and second rows, respectively.

$$\begin{aligned}
c &\equiv Y_{db}^u C - (Y_{db}^u + Y_{db}^c) P_{EW} , & c' &\equiv Y_{sb}^u \xi_c C - (Y_{sb}^u + Y_{sb}^c) P_{EW} , \\
p &\equiv -(Y_{db}^u + Y_{db}^c) \left(P - \frac{1}{3} P_{EW}^C \right) , & p' &\equiv -(Y_{sb}^u + Y_{sb}^c) \left(\xi_p P - \frac{1}{3} P_{EW}^C \right) , \\
s &\equiv -(Y_{db}^u + Y_{db}^c) \left(S - \frac{1}{3} P_{EW} \right) , & s' &\equiv -(Y_{sb}^u + Y_{sb}^c) \left(\xi_s S - \frac{1}{3} P_{EW} \right) , \\
a &\equiv Y_{db}^u A , & a' &\equiv Y_{sb}^u A , \\
e &\equiv Y_{db}^u E - (Y_{db}^u + Y_{db}^c) P A , & e' &\equiv Y_{sb}^u E - (Y_{sb}^u + Y_{sb}^c) P A ,
\end{aligned} \tag{2.4}$$

where $Y_{qb}^{q'} \equiv V_{q'q} V_{qb}^*$. Unless they are leading contributions, amplitudes such as e and pa are omitted from Tables 1 and 2.

One difference between the current analysis and our previous work [5] is that the CKM matrix elements associated with the amplitudes are factored out here. The strong phases, however, are still absorbed in the amplitudes. Notice that when going from $\Delta S = 0$ to $|\Delta S| = 1$ transitions, we explicitly include SU(3) breaking factors ξ_t, ξ_c , and ξ_p for the T, C , and P amplitudes, respectively. In the naive factorization

Mode	Flavor Amplitude	BR	\mathcal{A}_{CP}	
$B^- \rightarrow$	$\pi^- \bar{K}^0$	p'	23.1 ± 1.0	0.01 ± 0.02
	$\pi^0 K^-$	$-\frac{1}{\sqrt{2}}(p' + t' + c')$	12.8 ± 0.6	0.05 ± 0.03
	$K^- \eta$	$-\frac{1}{\sqrt{3}}(s' + t' + c')$	2.2 ± 0.4	-0.29 ± 0.11
	$K^- \eta'$	$\frac{1}{\sqrt{6}}(3p' + 4s' + t' + c')$	69.7 ± 2.8	0.03 ± 0.02
$\bar{B}^0 \rightarrow$	$\pi^+ K^-$	$-(p' + t')$	19.7 ± 0.6	-0.098 ± 0.015
	$\pi^0 \bar{K}^0$	$\frac{1}{\sqrt{2}}(p' - c')$	10.0 ± 0.6	-0.12 ± 0.11
				0.33 ± 0.21
	$\bar{K}^0 \eta$	$-\frac{1}{\sqrt{3}}(s' + c')$	1.2 ± 0.3	-
	$\bar{K}^0 \eta'$	$\frac{1}{\sqrt{6}}(3p' + 4s' + c')$	64.9 ± 4.4	-0.09 ± 0.06
			0.60 ± 0.08	
$\bar{B}_s^0 \rightarrow$	$K^+ K^-$	$-(p' + t')$	34 ± 9	-
	$K^0 \bar{K}^0$	p'	-	-
	$\pi^+ \pi^-$	$-(e' + pa')$	< 1.7	-
	$\pi^0 \pi^0$	$\frac{1}{\sqrt{2}}(e' + pa')$	-	-
	$\pi^0 \eta$	$-\frac{1}{\sqrt{6}}c'$	-	-
	$\pi^0 \eta'$	$-\frac{1}{\sqrt{3}}c'$	-	-
	$\eta \eta$	$-\frac{1}{3\sqrt{2}}(2p' - 2s' - 2c')$	-	-
	$\eta \eta'$	$\frac{1}{3\sqrt{2}}(4p' + 2s' - c')$	-	-
	$\eta' \eta'$	$\frac{1}{3\sqrt{2}}(4p' + 8s' + 2c')$	-	-

Table 2: Flavor amplitude decompositions for strangeness-changing $B \rightarrow PP$ decays. Measured branching ratios (in units of 10^{-6}) and CP asymmetries are given in the last two columns. For those modes with time-dependent CP asymmetries, \mathcal{A} and \mathcal{S} are listed in the first and second rows, respectively.

approximation, these SU(3) breaking factors are all equal to $\xi \equiv f_K/f_\pi = 1.223$ [11]. As an example, using the above-defined notations we have for the $B^0 \rightarrow K^+ \pi^-$ decay:

$$\mathcal{A}(K^+ \pi^-) = -Y_{sb}^u \xi_t T + (Y_{sb}^u + Y_{sb}^c) \xi_p P .$$

This can be obtained from the complete set of flavor amplitude decompositions given in Table 2.

The CKM factors used in the analysis are given in terms of the Wolfenstein parameterization of the CKM matrix to $O(\lambda^5)$. Since λ has been determined from kaon decays to a high accuracy, we will simply use the central value 0.2272 quoted by the CKMfitter group [2] as a theory input, and leave A , $\bar{\rho} \equiv \rho(1 - \lambda^2/2)$, and $\bar{\eta} \equiv \eta(1 - \lambda^2/2)$ as fitting parameters to be determined by data.

A relation between the sizes of EW penguin amplitude and tree-type amplitudes has been found in Ref. [12] where the Fierz transformation is used to relate EW

penguin operators with tree-level operators. Explicitly,

$$P_{EW} = -\delta_{EW}|T + C|e^{i\delta_{P_{EW}}} , \quad (2.5)$$

where $\delta_{P_{EW}}$ is the strong phase associated with P_{EW} . In the SM,

$$\delta_{EW} \simeq -\frac{3C_9 + C_{10}}{2C_1 + C_2} = 0.0135 \pm 0.0012 . \quad (2.6)$$

In our fit, we will leave it as a free parameter to test how well the above relation holds.

For the B meson decaying into a CP eigenstate f_{CP} , the time-dependent CP asymmetry is written as

$$\begin{aligned} A_{CP}(t) &= \frac{\Gamma(\bar{B}^0 \rightarrow f_{CP}) - \Gamma(B^0 \rightarrow f_{CP})}{\Gamma(\bar{B}^0 \rightarrow f_{CP}) + \Gamma(B^0 \rightarrow f_{CP})} \\ &= \mathcal{S} \sin(\Delta m_B \cdot t) + \mathcal{A} \cos(\Delta m_B \cdot t) , \end{aligned} \quad (2.7)$$

where Δm_B is the mass difference between the two mass eigenstates of B mesons and t is the decay time measured from the tagged B meson.

3. Fitting Analysis

To see the effects of SU(3) symmetry breaking, we consider the following four fitting schemes in our analysis:

1. exact flavor SU(3) symmetry for all amplitudes (*i.e.*, $\xi_t = \xi_c = \xi_p = 1$);
2. including the factor f_K/f_π for $|T|$ only (*i.e.*, $\xi_t = f_K/f_\pi$ and $\xi_c = \xi_p = 1$);
3. including the factor f_K/f_π for both $|T|$ and $|C|$ (*i.e.*, $\xi_t = \xi_c = f_K/f_\pi$ and $\xi_p = 1$); and
4. including a universal SU(3) breaking factor ξ for all amplitudes on top of Scheme 3 (*i.e.*, $\xi_t = \xi_c = \xi f_K/f_\pi$ and $\xi_p = \xi$).

To reduce the number of parameters, we assume exact flavor SU(3) symmetry for the strong phases in these fits. As a phase convention we set the tree amplitude to be real and positive, *i.e.*, $\delta_T = 0$.

In addition to the observables in $B \rightarrow PP$ modes, we also include $|V_{ub}| = (4.26 \pm 0.36) \times 10^{-3}$ and $|V_{cb}| = (41.63 \pm 0.65) \times 10^{-3}$ as our fitting observables. Here we take the averages of their values measured from inclusive and exclusive decays as quoted in Ref. [2]. They mainly help fixing the values of A and $\sqrt{\rho^2 + \eta^2}$. We will discuss below how our fit results and predictions change should we use a lower value of V_{ub} in the following numerical analysis.

3.1 Fits to modes with only π, K mesons in the final state

We start by fitting to the branching ratios and CP asymmetries of the $\pi\pi$, πK , and KK modes of B meson decays. This part of the analysis avoid uncertainties in the wave functions and singlet amplitudes associated with the η and η' mesons.

Currently, there are 20 experimental observables. Along with $|V_{ub}|$ and $|V_{cb}|$ mentioned above, we have totally 22 data points. The number of theoretical parameters is 10 for Schemes 1 to 3 and 11 for Scheme 4. The best-fitted values of the parameters in their 1σ ranges along with the minimal χ^2 values, χ^2_{\min} , for the different schemes are listed in Table 3.

Parameter	Scheme 1	Scheme 2	Scheme 3	Scheme 4
$\bar{\rho}$	$0.139^{+0.042}_{-0.037}$	$0.134^{+0.041}_{-0.036}$	$0.134^{+0.041}_{-0.036}$	$0.133^{+0.039}_{-0.035}$
$\bar{\eta}$	0.401 ± 0.030	0.403 ± 0.031	0.404 ± 0.031	0.399 ± 0.031
A	0.807 ± 0.013	0.807 ± 0.013	0.807 ± 0.013	0.807 ± 0.013
$ T $	$0.573^{+0.055}_{-0.047}$	$0.575^{+0.055}_{-0.047}$	$0.574^{+0.055}_{-0.047}$	$0.582^{+0.056}_{-0.049}$
$ C $	0.371 ± 0.050	0.364 ± 0.050	0.364 ± 0.049	0.372 ± 0.051
δ_C	-57.6 ± 10.3	-55.9 ± 10.7	-55.8 ± 10.2	-56.3 ± 10.1
$ P $	0.121 ± 0.002	0.122 ± 0.002	0.122 ± 0.002	0.117 ± 0.008
δ_P	-22.7 ± 4.0	-18.8 ± 3.2	-19.3 ± 3.2	$-18.6^{+3.2}_{-3.5}$
$ P_{EW} $	$0.011^{+0.006}_{-0.003}$	$0.011^{+0.006}_{-0.003}$	$0.011^{+0.005}_{-0.003}$	$0.011^{+0.004}_{-0.003}$
$\delta_{P_{EW}}$	$-4.3^{+34.1}_{-50.6}$	$2.2^{+32.0}_{-49.3}$	$-10.0^{+37.2}_{-45.3}$	-15.1 ± 39.9
ξ	1(fixed)	1(fixed)	1(fixed)	$1.04^{+0.08}_{-0.07}$
δ_{EW}	0.013 ± 0.006	0.013 ± 0.006	0.013 ± 0.005	0.013 ± 0.004
χ^2_{\min}/dof	18.9/12	18.0/12	16.4/12	16.1/11

Table 3: Fit results of the parameters for the $\pi\pi$, πK , and KK modes in Schemes 1 through 4 defined in the text along with the minimal χ^2 value. The amplitudes are given in units of 10^4 eV.

Generally speaking, we obtain fairly stable results for the parameters, except for some small variations in the strong phases among the SU(3) breaking schemes considered here. The fit quality is best in Scheme 3, suggesting that it is better to include the SU(3) breaking factor f_K/f_π for the T and C amplitudes when going from the strangeness-conserving modes to the strangeness-changing modes. Scheme 4 introduces an additional SU(3) breaking factor ξ , which is found to be about 1.04. The small difference in χ^2_{\min} between Scheme 3 and Scheme 4 turns out to reduce the fitting quality from 17% down to 14%.

It has been suggested as a direct test of flavor SU(3) symmetry by comparing the extracted amplitude magnitudes of $B^0 \rightarrow K^0 \bar{K}^0$ and $B^+ \rightarrow K^+ \bar{K}^0$ with $B^+ \rightarrow K^0 \pi^+$ because all of them have the same single penguin amplitude contributing to the decays, except for the only difference in the CKM factors. This is verified

experimentally according to the current data. Taking the averaged invariant amplitudes of $\bar{B}^0 \rightarrow K^0 \bar{K}^0$ and $B^- \rightarrow K^- \bar{K}^0$ as $|p|$ and comparing it with $|p'|$ obtained from $B^+ \rightarrow K^0 \pi^+$, one obtains $|p/p'| \simeq 0.23 \pm 0.02$ consistent with the expected ratio $|V_{cd}/V_{cs}|$. This justifies our choice of not including the factor f_K/f_π for SU(3) breaking in the penguin amplitudes. We also find that χ_{\min}^2 becomes worse when the factor is imposed on the QCD penguin amplitude. Therefore, the data indicate that to a good approximation factorization works better for the color-allowed and color-suppressed tree amplitudes (*i.e.*, T and C).

We observe a large $|C|/|T|$ ratio of about 0.63 in all these fits. This is different from the expectation of the usual perturbative calculation within the SM. A possible explanation is given in Ref. [13] where next-to-leading order corrections to the interaction vertex are found to enhance the color-suppressed amplitude C for $K\pi$ decays by a factor of 2 to 3 while keeping other amplitudes more or less unchanged. Moreover, there exists a large relative strong phase of about $(-56 \pm 10)^\circ$ between C and T . Therefore, it can play an important role in CP asymmetries. The values of these parameters are largely driven by the large branching ratio of $\pi^0 \pi^0$ and $A_{CP}(\pi^0 K^-)$ being quite different from $A_{CP}(\pi^+ K^-)$.

A strong phase of about -20° is associated with the penguin amplitude. This is primarily demanded by the CP asymmetries of the $\pi^+ \pi^-$ and $K^+ \pi^-$ modes, both of which involve the combination of $t^{(\prime)}$ and $p^{(\prime)}$.

In all our fits, the parameter δ_{EW} is seen to be very stable and close to the value in Eq. (2.6), which shows that the EW penguin amplitude has a size roughly agreeing with the SM expectation. This is partly due to the fact that the latest data are moving towards the SM estimates and a larger best fitted γ is favored, modifying the $T - P$ and $T - P_{EW}$ interferences and enhancing $Br(\pi^0 \bar{K}^0)$. It does not necessarily mean that the possibility of new physics has been ruled out. As it will be shown below (see Section 3.3), an electroweak penguin-like new contribution with a different CP phase can dramatically improve the quality of fits. Besides, we find that P_{EW} has a strong phase of about -10° relative to T and about 45° to C .

Since the 1σ and 95%CL ranges for the $(\bar{\rho}, \bar{\eta})$ vertex have unnoticeable change in the four fitting schemes defined above, we only present as a representative our preferred set, Scheme 3, in Fig. 1. This also shows the stability of the $(\bar{\rho}, \bar{\eta})$ values against SU(3) breaking. Scheme 3 gives the following results for the weak phases α , β , and γ :

$$\begin{aligned} \alpha &= (83_{-7}^{+6})^\circ, \quad \text{or} \quad 69^\circ \leq \alpha \leq 96^\circ \quad (95\% \text{ CL}); \\ \beta &= (26 \pm 2)^\circ, \quad \text{or} \quad 21^\circ \leq \beta \leq 31^\circ \quad (95\% \text{ CL}); \\ \gamma &= (72_{-5}^{+4})^\circ, \quad \text{or} \quad 62^\circ \leq \gamma \leq 81^\circ \quad (95\% \text{ CL}). \end{aligned} \tag{3.1}$$

As shown in Fig. 1, the determined ranges of $(\bar{\rho}, \bar{\eta})$ for all the schemes in our fitting are slightly higher than those given by the latest CKMfitter and UTfit results

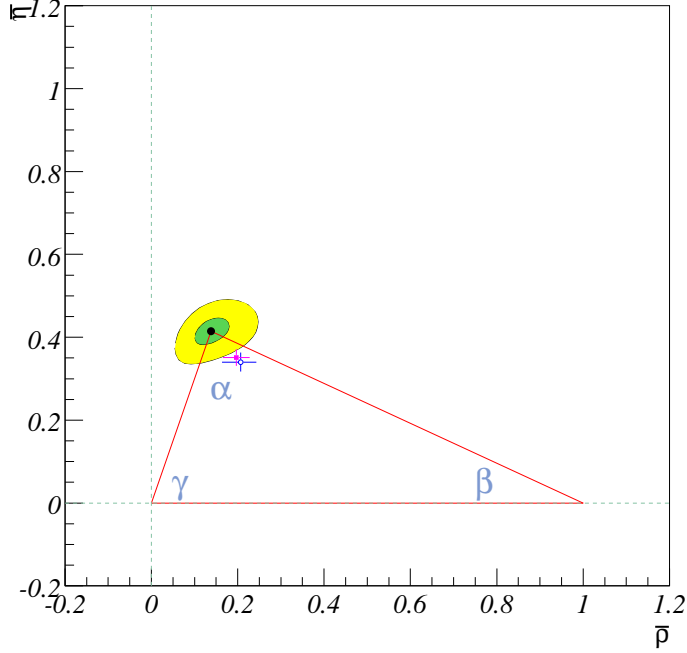


Figure 1: Constraints on the $(\bar{\rho}, \bar{\eta})$ vertex using $B \rightarrow \pi\pi, K\pi$, and KK data in Scheme 3 defined in the text. Contours correspond to 1σ and 95% CL, respectively. The crosses refer to the 1σ range given by the latest CKMfitter (open circle) and UTfit (filled square) results using other methods [2, 3] as a comparison.

obtained using other observables [2, 3]:

$$\begin{aligned}
 \text{CKMfitter: } \bar{\rho} &= 0.207_{-0.034}^{+0.036}, \quad \bar{\eta} = 0.341 \pm 0.023; \\
 \text{UTfit: } \bar{\rho} &= 0.197 \pm 0.031, \quad \bar{\eta} = 0.351 \pm 0.020.
 \end{aligned}
 \tag{3.2}$$

These values are indicated by crosses with an open circle and a filled square in the figure, respectively. The difference is to a large extent caused by the large value of $|V_{ub}|$ used in our fits. Therefore, we obtain slightly larger phases β and γ but a smaller α .

We now briefly comment on the effects of using a smaller value of $|V_{ub}|$ in the fits. If we take $|V_{ub}| = (3.50 \pm 0.18) \times 10^{-3}$ extracted from unitarity angle measurements only [38], χ_{\min}^2 is improved by 1.1. β reduces to around 21° and γ increases to about 75° , with α almost unaffected. The magnitudes of $|T|$ and $|C|$ both become slightly larger, but their ratio stays the same. The other parameters do not change much either. The same features are also observed in fits with all PP modes to be discussed in the next section. However, it should be emphasized that our analysis purposely avoid inputs other than the charmless decay modes unless necessary (such as λ and $|V_{cb}|$ mentioned above). We therefore do not use this smaller $|V_{ub}|$ value in our main analysis, for it relies quite a lot on charmed B decays.

Our predictions for the branching ratios and CP asymmetries for all the $B_{u,d} \rightarrow \pi\pi, K\pi$, and KK modes based upon the extracted parameters in Table 3 are given in Table 4.

Observable	Scheme 1	Scheme 2	Scheme 3	Scheme 4
$Br(\pi^+\pi^-)$	5.4 ± 1.1	5.4 ± 1.0	5.3 ± 1.0	5.3 ± 1.1
$Br(\pi^0\pi^0)$	1.6 ± 0.4	1.6 ± 0.4	1.6 ± 0.4	1.5 ± 0.4
$Br(\pi^-\pi^0)$	5.3 ± 1.2	5.4 ± 1.2	5.4 ± 1.2	5.4 ± 1.3
$Br(\pi^+K^-)$	20.2 ± 1.0	20.1 ± 1.1	20.1 ± 1.1	20.3 ± 4.3
$Br(\pi^0\bar{K}^0)$	9.9 ± 1.0	9.9 ± 1.0	10.0 ± 0.9	10.1 ± 2.3
$Br(\pi^-\bar{K}^0)$	23.0 ± 1.1	23.1 ± 1.1	23.1 ± 1.1	23.4 ± 4.8
$Br(\pi^0K^-)$	12.0 ± 1.2	12.1 ± 1.2	12.0 ± 1.1	12.2 ± 2.5
$Br(K^+K^-)$	0	0	0	0
$Br(K^0\bar{K}^0)$	1.0 ± 0.1	1.0 ± 0.1	1.0 ± 0.1	1.0 ± 0.2
$Br(K^-\bar{K}^0)$	1.1 ± 0.1	1.1 ± 0.1	1.1 ± 0.1	1.0 ± 0.2
$\mathcal{A}(\pi^+\pi^-)$	0.32 ± 0.07	0.27 ± 0.06	0.28 ± 0.06	0.26 ± 0.06
$\mathcal{A}(\pi^0\pi^0)$	0.47 ± 0.15	0.49 ± 0.15	0.49 ± 0.14	0.50 ± 0.14
$A_{CP}(\pi^-\pi^0)$	-0.01 ± 0.04	-0.02 ± 0.03	-0.01 ± 0.03	-0.01 ± 0.03
$A_{CP}(\pi^+K^-)$	-0.08 ± 0.02	-0.09 ± 0.02	-0.09 ± 0.02	-0.09 ± 0.02
$\mathcal{A}(\pi^0K_S)$	-0.07 ± 0.03	-0.08 ± 0.02	-0.09 ± 0.03	-0.10 ± 0.03
$A_{CP}(\pi^-\bar{K}^0)$	0	0	0	0
$A_{CP}(\pi^0K^-)$	0.00 ± 0.03	0.00 ± 0.03	0.01 ± 0.04	0.02 ± 0.04
$A_{CP}(K^+K^-)$	0	0	0	0
$\mathcal{A}(K^0\bar{K}^0)$	0	0	0	0
$A_{CP}(K^-\bar{K}^0)$	0	0	0	0
$\mathcal{S}(\pi^+\pi^-)$	-0.580 ± 0.130	-0.585 ± 0.130	-0.584 ± 0.130	-0.565 ± 0.141
$\mathcal{S}(\pi^0\pi^0)$	0.814 ± 0.109	0.812 ± 0.108	0.810 ± 0.106	0.786 ± 0.113
$\mathcal{S}(\pi^0K_S)$	0.851 ± 0.042	0.850 ± 0.041	0.861 ± 0.041	0.858 ± 0.042
$\mathcal{S}(K^0\bar{K}^0)$	-0.000 ± 0.014	-0.000 ± 0.014	-0.000 ± 0.014	-0.000 ± 0.015

Table 4: Predicted branching ratios (in units of 10^{-6}) and CP asymmetries for $B \rightarrow \pi\pi, K\pi$, and KK modes in different schemes. The observables with vanishing entries are predicted to be identically zero in our analysis. Experimentally measured quantities, if any, are already given in the last two columns of Tables 1 and 2 for comparison.

It is seen that the values in the table are quite stable and generally in agreement with the measured numbers or upper bounds within the errors. The largest χ^2 comes from $\mathcal{S}(\pi^0K_S)$, which is entailed to be even larger than $\mathcal{S}_{(c\bar{c})K_S}$. The CP asymmetry of $K^-\pi^0$ is found to be close to zero, giving the second largest contribution to χ^2 . As we will see in Section 3.3, these discrepancies can be significantly reduced if a new amplitude is introduced.

The central values of $\mathcal{A}(\pi^+\pi^-)$ are slightly smaller than the measured one, but deviate from zero at more than 4σ level. The predicted $\mathcal{A}(\pi^0\pi^0)$ are noticeably different from zero. This is seen as a result of the absence of a dominant amplitude in the decay. We also find a sizeable $\mathcal{S}(\pi^0\pi^0) \sim 0.8 \pm 0.1$, to be verified experimentally.

At this point, it may be helpful to compare the predictions of other approaches. The recent next-to-leading order (NLO) calculations in QCD factorization (QCDF) show some enhancements from strong penguin corrections at $\mathcal{O}(\alpha_s^2)$ [39]. However, their predictions for CP-averaged decay rates of the πK modes still tend to be lower than the experimental data using the default parameter set, and the observed large negative $A_{CP}(\pi^+K^-)$ is difficult to understand. The hard spectator-scattering corrections have also been calculated to this order, and are found to possibly have a significant impact on the tree-dominated $B \rightarrow \pi\pi$ decays [40]. It remains to be seen if a complete next-to-next-to-leading order (NNLO) calculation can lead to a better agreement with the data.

In the perturbative QCD (pQCD) approach, NLO calculations including vertex corrections, quark loops and magnetic penguins suppress $A_{CP}(\pi^0K^-)$ while keep $A_{CP}(\pi^+K^-)$ large enough with the correct sign [13], both in good agreement with the data. Nevertheless, the corrections to $\pi\pi$ modes are ineffective so that the predicted $Br(\pi^0\pi^0)$ remains small.

A recent comprehensive analysis in the same set of observables has been performed in the heavy quark limit of QCD and in the soft-collinear effective theory (SCET) [42]. This approach generally involves more hadronic parameters without the help of symmetries. At the LO, they predict a larger $Br(\pi^+K^-)$, an $A_{CP}(\pi^0K^-)$ close to $A_{CP}(\pi^+K^-)$, and an $\mathcal{A}(\pi^0\bar{K}^0)$ opposite in sign to the data.

In all these approaches, the predicted $S(\pi^0K_S)$ are close to the one from $S(J/\psi K_S)$ or even larger [41, 13, 42]. This leaves room for new physics interpretations if it is further confirmed by data at a higher precision.

Our predictions for the branching ratios and CP asymmetries for all the $B_s \rightarrow \pi\pi, K\pi,$ and KK modes based upon the extracted parameters in Table 3 are given in Table 5. They serve as another good testing ground for the flavor SU(3) symmetry. Among all observables of the B_s decays only the branching ratio of the $B_s \rightarrow K^+K^-$ mode is observed at CDF [35]. This mode has the same flavor amplitude decomposition as the $\bar{B}^0 \rightarrow \pi^+K^-$ mode. Therefore, our predictions in this case are close to those for $\bar{B}^0 \rightarrow \pi^+K^-$, apart from a small difference due to such factors as the masses and decay widths. They are all smaller than the measured value. Since this is only observed for the first time with somewhat large errors, a more precise determination will be very helpful. Besides, this mode is predicted to have nonzero CP asymmetries according to the fits.

As mentioned above, a good flavor SU(3) symmetry relation has been observed between $\bar{B}^0 \rightarrow K^0\bar{K}^0$ and $B^- \rightarrow \pi^-\bar{K}^0$. It is therefore natural to use the $B_s \rightarrow K^0\bar{K}^0$ decay as another test because it also involves a single p' amplitude. We

Observable	Scheme 1	Scheme 2	Scheme 3	Scheme 4
$Br(\pi^+\pi^-)$	0	0	0	0
$Br(\pi^0\pi^0)$	0	0	0	0
$Br(\pi^+K^-)$	5.0 ± 1.0	5.0 ± 1.0	5.0 ± 1.0	5.0 ± 1.0
$Br(\pi^0K^0)$	1.5 ± 0.3	1.5 ± 0.3	1.5 ± 0.3	1.4 ± 0.3
$Br(K^+K^-)$	18.9 ± 1.0	18.8 ± 1.0	18.8 ± 1.0	19.0 ± 4.0
$Br(K^0\bar{K}^0)$	20.0 ± 1.0	20.2 ± 1.0	20.1 ± 1.0	20.4 ± 4.2
$\mathcal{A}(\pi^+\pi^-)$	0	0	0	0
$\mathcal{A}(\pi^0\pi^0)$	0	0	0	0
$A_{CP}(\pi^+K^-)$	0.32 ± 0.07	0.27 ± 0.06	0.28 ± 0.06	0.26 ± 0.06
$\mathcal{A}(\pi^0K_S)$	0.47 ± 0.15	0.49 ± 0.15	0.49 ± 0.14	0.50 ± 0.14
$\mathcal{A}(K^+K^-)$	-0.08 ± 0.02	-0.09 ± 0.02	-0.09 ± 0.02	-0.09 ± 0.02
$\mathcal{A}(K^0\bar{K}^0)$	0	0	0	0
$\mathcal{S}(\pi^+\pi^-)$	0	0	0	0
$\mathcal{S}(\pi^0\pi^0)$	0	0	0	0
$\mathcal{S}(\pi^0K_S)$	0.340 ± 0.202	0.365 ± 0.194	0.359 ± 0.193	0.308 ± 0.201
$\mathcal{S}(K^+K^-)$	0.147 ± 0.022	0.199 ± 0.028	0.198 ± 0.028	0.211 ± 0.035
$\mathcal{S}(K^0\bar{K}^0)$	-0.043 ± 0.004	-0.044 ± 0.004	-0.044 ± 0.004	-0.043 ± 0.004

Table 5: Predicted branching ratios (in units of 10^{-6}) and CP asymmetries for B_s decays in different schemes. The observables with vanishing entries are predicted to be identically zero in our analysis.

predict its branching ratio to be around 2×10^{-5} . Moreover, the time-dependent CP asymmetries \mathcal{A} and \mathcal{S} associated with this mode are predicted to be identically zero and about -0.044 ± 0.004 , respectively. The $B_s \rightarrow K^0\bar{K}^0$ and K^+K^- decays have also been discussed in the literature to study their correlation with the $B_d \rightarrow \pi^+\pi^-$ decay [43] and their time-dependent CP asymmetries for identifying new physics [44] if they deviate from the SM predictions.

The $B_s \rightarrow K^-\pi^+$ and K^+K^- modes have the same flavor amplitude decompositions as the $\bar{B}^0 \rightarrow \pi^+\pi^-$ and π^+K^- decays, respectively. Therefore, they are predicted to have sizeable CP asymmetries due to the interference between tree and penguin amplitudes.

The same color-suppressed and penguin amplitudes contribute to both $\bar{B}^0 \rightarrow \pi^0\pi^0$ and $\bar{B}_s \rightarrow \pi^0K^0$ modes. Neither of them is dominant in the decay processes. Therefore, we expect large CP asymmetries in the latter mode as well. Moreover, determining the branching ratio of the latter may provide some insight for the observed large branching ratio of the former.

3.2 Fits to all $B \rightarrow PP$ modes

We further carry out the analysis with the inclusion of modes with η and η' in the final state. In this case, there are totally 34 experimental observables. The best fitted parameters are listed in Table 6.

Parameter	Scheme 1	Scheme 2	Scheme 3	Scheme 4
$\bar{\rho}$	$0.089^{+0.031}_{-0.027}$	$0.087^{+0.029}_{-0.026}$	$0.087^{+0.029}_{-0.026}$	$0.096^{+0.029}_{-0.026}$
$\bar{\eta}$	0.377 ± 0.027	0.378 ± 0.028	0.379 ± 0.027	0.370 ± 0.027
A	0.809 ± 0.012	0.809 ± 0.012	0.809 ± 0.012	0.809 ± 0.012
$ T $	$0.641^{+0.056}_{-0.050}$	$0.642^{+0.056}_{-0.050}$	$0.640^{+0.056}_{-0.049}$	$0.649^{+0.056}_{-0.049}$
$ C $	0.426 ± 0.048	0.418 ± 0.048	0.415 ± 0.047	0.436 ± 0.049
δ_C	-72.5 ± 7.3	-70.4 ± 7.5	-70.0 ± 7.3	-68.3 ± 7.2
$ P $	0.121 ± 0.002	0.121 ± 0.002	0.121 ± 0.002	0.110 ± 0.008
δ_P	-17.8 ± 3.2	-16.0 ± 2.8	-16.4 ± 2.8	-15.9 ± 2.6
$ P_{EW} $	$0.012^{+0.006}_{-0.004}$	$0.011^{+0.005}_{-0.003}$	$0.012^{+0.006}_{-0.004}$	$0.013^{+0.006}_{-0.004}$
$\delta_{P_{EW}}$	$-58.8^{+39.8}_{-20.6}$	$-47.7^{+42.9}_{-24.9}$	$-58.1^{+35.9}_{-19.3}$	$-57.6^{+32.5}_{-18.2}$
$ S $	$0.048^{+0.004}_{-0.003}$	$0.047^{+0.004}_{-0.003}$	$0.047^{+0.003}_{-0.003}$	0.042 ± 0.004
δ_S	-48.3 ± 10.6	-44.8 ± 10.2	-44.2 ± 9.8	-42.9 ± 9.3
ξ	1(fixed)	1(fixed)	1(fixed)	$1.10^{+0.09}_{-0.07}$
δ_{EW}	0.014 ± 0.006	0.013 ± 0.005	0.014 ± 0.006	0.015 ± 0.006
χ^2/dof	37.4/22	34.8/22	32.9/22	30.6/21

Table 6: Fit results of the parameters for all PP modes in Schemes 1 through 4 defined in the text along with the associated minimal χ^2 values. The amplitudes are given in units of 10^4 eV.

To fit all the PP modes, we have to include at least the flavor singlet amplitude S , whose importance for explaining the large branching ratios of the $\eta'K$ modes has been noticed and discussed in Refs. [45, 46, 47]. This introduces two more theoretical parameters $|S|$ and δ_S , the strong phase associated with S , than the fits in Section 3.1. However, the fitting quality in these schemes is seen to be much worse than before. Among the modes with $\eta^{(\prime)}$ in the final state, $Br(\eta K^-)$, $S_{\eta'K_S}$, and $A_{CP}(\pi^- \eta')$ have the largest contributions to χ^2 .

Comparing the fitting results in Table 6 with those in Table 3, we see that the strong phases suffer from larger fluctuations among all theoretical parameters. The values of both $\bar{\rho}$ and $\bar{\eta}$ are decreased, but their precisions improved. This leaves a smaller region for the $(\bar{\rho}, \bar{\eta})$ vertex, with a β consistent with other observations and a somewhat larger γ . The parameters $|T|$ and $|C|$ become slightly larger; but the ratio $|C|/|T| \sim 0.65$ remains about the same. The magnitudes of P and P_{EW} (or δ_{EW}) are seen to be relatively stable in both limited and global fits. The parameter ξ increases from 1.04 to 1.10.

The singlet amplitude has a magnitude about 3 to 4 times $|P_{EW}|$ in our fits. Moreover, its strong phase is close to $\delta_{P_{EW}}$ and about -30° from P . It is this feature that produces interesting interference patterns among the different modes involving η and η' .

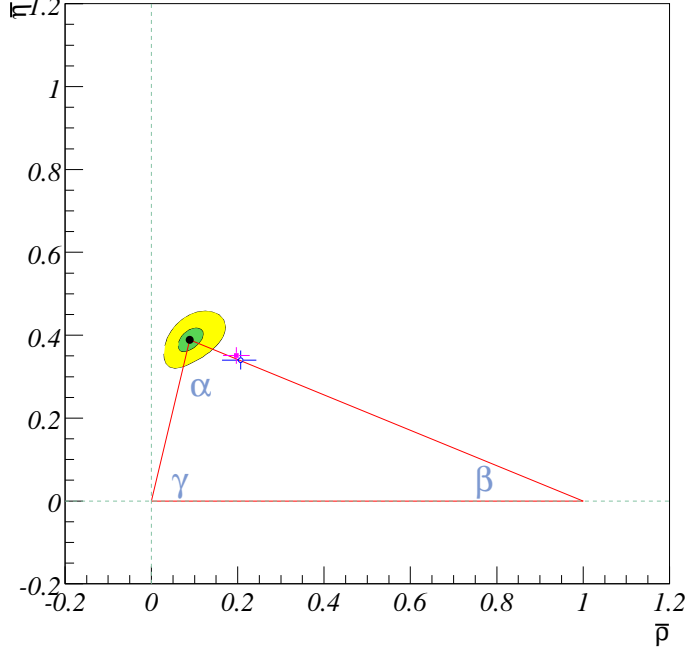


Figure 2: Constraints on the $(\bar{\rho}, \bar{\eta})$ vertex using all the PP mode data in Scheme 3 defined in the text. Contours correspond to 1σ and 95% CL, respectively. The crosses refer to the 1σ range given by the latest CKMfitter (open circle) and UTfit (filled square) results using other methods [2, 3] as a comparison.

Scheme 3 in this case gives the following results for the weak phases α , β , and γ :

$$\begin{aligned}
 \alpha &= (80 \pm 6)^\circ, \quad \text{or} \quad 69^\circ \leq \alpha \leq 92^\circ \quad (95\% \text{ CL}) ; \\
 \beta &= (23 \pm 2)^\circ, \quad \text{or} \quad 20^\circ \leq \beta \leq 27^\circ \quad (95\% \text{ CL}) ; \\
 \gamma &= (77 \pm 4)^\circ, \quad \text{or} \quad 69^\circ \leq \gamma \leq 84^\circ \quad (95\% \text{ CL}) .
 \end{aligned}
 \tag{3.3}$$

The predictions of the $B_{u,d}$ decay observables are given in Table 7. Vanishing observables in our approach are omitted to avoid an oversized table. The following observables deviate the most from the current data: $\mathcal{S}(\pi^0 K_S)$, $Br(\pi^-\pi^0)$, $Br(K^-\eta)$, $Br(\pi^0\pi^0)$, $\mathcal{S}(\eta' K_S)$, and $A_{CP}(\pi^-\eta)$ (listed in the order of their contributions to χ^2).

As in the limited fits in Section 3.1, the global fits also prefer sizeable CP asymmetries for the $\pi^0\pi^0$ and $\pi^+\pi^-$ modes. The branching ratios of the yet measured $\eta\eta$, $\eta\eta'$, and $\eta'\eta'$ are all consistent with the current upper bounds. Their corresponding

direct CP asymmetries are predicted to be large. However, measuring them will require more work.

The current branching ratios of $\pi^0\eta$ and $\pi^0\eta'$ has a factor of 2 difference in the central values, though the errors are still large. Our results, on the other hand, show that they are equal to each other in all schemes. $\mathcal{A}(\eta K_S)$ has not been observed, but is 2σ away from zero in our analysis.

The predictions for the B_s modes are given in Table 8. Many of the discussions regarding the modes with π and K mesons in the final state in Section 3.1 can be applied here. Thus, we only concentrate on the modes with η and/or η' in the final state.

As in the cases of $\bar{B}^0 \rightarrow \eta' K_S$ and $B^- \rightarrow K^- \eta'$, the constructive interference between p' and s' makes the $\bar{B}_s^0 \rightarrow \eta' \eta'$ the one with the largest branching ratio, $\sim 50 \times 10^{-6}$, among all. The same effect is seen in the $\bar{B}_s^0 \rightarrow \eta \eta'$ decay as well. In contrast, a destructive effect occurs in the $\bar{B}_s^0 \rightarrow \eta \eta$ decay, so that its branching ratio is only $\sim 2 \times 10^{-6}$.

The $\bar{B}_s^0 \rightarrow \eta' K_S$ decay is another place where the constructive interference between the QCD penguin and singlet penguin amplitudes plays an important role. Although small in magnitude for $\Delta S = 0$ transitions, they can interfere with the color-suppressed amplitude to give potentially observable time-dependent CP asymmetries, both predicted at $\sim 5\sigma$ level.

3.3 Fits with a new physics amplitude

In expectation of possible new physics contributions to the $K\pi$ decays to account for the observed branching ratio and CP violation pattern [48, 49, 50, 51, 52], we try in Scheme 3 fits with a new amplitude added to these decays. More explicitly, a new amplitude $N = |N| \exp[i(\phi_N + \delta_N)]$ is included in the $B \rightarrow \pi^0 K^-$ and $\pi^0 \bar{K}^0$ decays in such a way that effectively,

$$c' \rightarrow Y_{sb}^u \xi_c C - (Y_{sb}^u + Y_{sb}^c) P_{EW} + N . \quad (3.4)$$

This introduces three more parameters ($|N|$, ϕ_N , and δ_N) into the fits. Here we assume that P_{EW} is fixed relative to $T + C$ through the SM relation. χ_{\min}^2 is found to decrease from 16.4 to 4.3 in the limited fit with only π , K mesons in the final state. The new physics parameters are found to be

$$|N| = 18_{-4}^{+3} \text{ eV} , \quad \phi_N = (92 \pm 4)^\circ , \quad \text{and} \quad \delta_N = (-14 \pm 5)^\circ . \quad (3.5)$$

The best fitted CKM parameters $\bar{\rho}$, $\bar{\eta}$ and A remain almost unchanged. The best fitted tree-type amplitudes have $|T| = (0.55_{-0.04}^{+0.05}) \times 10^4 \text{ eV}$, $|C| = (0.32_{-0.04}^{+0.05}) \times 10^4 \text{ eV}$ and $\delta_C = (-39_{-13}^{+16})^\circ$. The penguin amplitude $|P|$ is unchanged.

Since both C and P_{EW} have the same flavor topology, they always appear in pairs in c or c' for any physical decay process. Therefore, it seems difficult to determine

whether the new amplitude is associated with one or the other [53]. Our results have $|N|/|V_{cb}V_{cs}| \simeq 0.04 \times 10^4 \text{eV}$ and $|N|/|V_{ub}V_{us}| \simeq 2.2 \times 10^4 \text{eV}$, showing that the new amplitude is unexpectedly large. It is about five times bigger than $|P_{EW}|$ or $|C|$. Since we assume that it only enters c' in the $K\pi$ modes instead of c in the $\pi\pi$ modes, this result suggests that it behaves more like the electroweak penguin amplitude than the color-suppressed amplitude, for the former plays a much less important role than the latter in the strangeness-conserving modes. Although the latest data indicate only a mild deviation of πK branching ratios from SM estimates, the large difference between $A_{CP}(\pi^+K^-)$ and $A_{CP}(\pi^0K^-)$ is unexpected, which require a much larger $|C'|/|T'|$ than $|C|/|T|$ in $\pi\pi$ modes [54]. Within the framework of SU(3) symmetry, a large new physics contribution is still possible.

The above conclusion may look contradictory to what we have found in Section 3.1, where $|P_{EW}|$ is preferred by data to fall within the SM expectation, meaning that varying its value would not improve the fitting quality. But this is only because in the previous fit, the weak phase of P_{EW} is fixed to the SM value. In the analysis of this section, the electroweak penguin-like new amplitude N is allowed to have its own weak and strong phases.

It should be emphasized that N is not added to modes with the contributing amplitude c' in the global fits other than the $K\pi$ decays. It does not improve the minimal χ^2 much to do so, for there is a pull between the $K\pi$ and $K\eta^{(\prime)}$ data such that $|N|$ is about a factor of 5 smaller than that quoted above. Therefore, it remains to be understood why the new amplitude does not help when modes with η and η' are taken into consideration as it should if flavor SU(3) is respected. The solution to this question may rely on more precisely determined branching ratios of $\eta K^{0,-}$.

4. Summary

In this paper, we perform χ^2 fits to the branching ratios and CP asymmetries of both limited and entire sets of the rare $B \rightarrow PP$ decays. We consider the primary contributing flavor amplitudes T , C , P , and P_{EW} , each of which is associated with a distinct strong phase. The analysis is based upon flavor SU(3) symmetry. We also include the f_K/f_π ratio and an additional SU(3) breaking factor ξ to test the stability of our fits.

One major result is the extraction of the vertex $(\bar{\rho}, \bar{\eta})$ and thus the weak phases of the CKM unitarity triangle. This is complementary to other methods. The values of β and γ obtained from our fits for modes without $\eta^{(\prime)}$ in the final state are generally larger than but still consistent within errors with those given by the overall fits of the CKMfitter and UTfit groups to other observables. Our fits to all the PP modes, however, result in a β similar to that given by both the CKMfitter and the UTfit groups but a larger γ .

The current PP data favor a large C with a strong phase of about -60° with respect to T . This is seen to be required by the large branching ratio of $\pi^0\pi^0$ and the fact that $A_{CP}(\pi^0K^-)$ is different from $A_{CP}(\pi^+K^-)$. On the other hand, the size of electroweak penguin amplitude P_{EW} is found to be consistent with the SM expectation.

We also comment on the possibility of a new physics contribution to $K\pi$ decays. Our fitting analysis in this case prefers an electroweak penguin-like amplitude with sizeable magnitude and nontrivial weak phase given in Eq. (3.5). However, this amplitude does not respect flavor $SU(3)$ symmetry.

Using the parameters extracted from fitting, we make predictions for all the rare $B \rightarrow PP$ processes. Moreover, we extend our predictions to the observables in B_s decays based on flavor $SU(3)$ symmetry, whose experimental data will become available for comparison in the next couple of years from Tevatron Run II, LHCb and upgraded Belle experiments.

Acknowledgments

C.-W. C. would like to thank the hospitality of the KEK Theory Group during his visit where this work was initiated and that of the National Center for Theoretical Sciences in Hsinchu. He also thanks N. Deshpande for helpful discussions and the hospitality of the Institute of Theoretical Science at Univ. of Oregon during his visit. This research was supported in part by the National Science Council of Taiwan, R.O.C. under Grant No. NSC 94-2112-M-008-023-. Y.-F. Z. is supported by JSPS foundation.

References

- [1] N. Cabibbo, Phys. Rev. Lett. **10**, 531 (1963); M. Kobayashi and T. Maskawa, Prog. Theor. Phys. **49**, 652 (1973).
- [2] J. Charles *et al.* [CKMfitter Group], Eur. Phys. J. C **41**, 1 (2005) [arXiv:hep-ph/0406184]. Updated results may be found on the web site: <http://ckmfitter.in2p3.fr/>.
- [3] M. Bona *et al.* [UTfit Collaboration], JHEP **0507**, 028 (2005) [arXiv:hep-ph/0501199]. Updated results may be found on the web site: <http://utfit.roma1.infn.it/>.
- [4] M. Beneke, G. Buchalla, M. Neubert and C. T. Sachrajda, Nucl. Phys. B **606**, 245 (2001) [hep-ph/0104110]; M. Beneke and M. Neubert, Nucl. Phys. B **651**, 225 (2003) [hep-ph/0210085]; M. Beneke and M. Neubert, Nucl. Phys. B **675**, 333 (2003) [arXiv:hep-ph/0308039].

- [5] C. W. Chiang, M. Gronau, Z. Luo, J. L. Rosner and D. A. Suprun, Phys. Rev. D **69**, 034001 (2004) [arXiv:hep-ph/0307395]; C. W. Chiang, M. Gronau, J. L. Rosner and D. A. Suprun, Phys. Rev. D **70**, 034020 (2004) [arXiv:hep-ph/0404073].
- [6] Y. F. Zhou, Y. L. Wu, J. N. Ng and C. Q. Geng, Phys. Rev. D **63**, 054011 (2001) [arXiv:hep-ph/0006225]; X. G. He, Y. K. Hsiao, J. Q. Shi, Y. L. Wu and Y. F. Zhou, Phys. Rev. D **64**, 034002 (2001) [arXiv:hep-ph/0011337]; H. K. Fu, X. G. He, Y. K. Hsiao and J. Q. Shi, Nucl. Phys. Proc. Suppl. **115**, 279 (2003) [arXiv:hep-ph/0210243]; Y. L. Wu and Y. F. Zhou, Eur. Phys. J. directC **5**, 014 (2003) [arXiv:hep-ph/0210367].
- [7] Y. L. Wu and Y. F. Zhou, Phys. Rev. D **71**, 021701 (2005) [arXiv:hep-ph/0409221]; Phys. Rev. D **72**, 034037 (2005) [arXiv:hep-ph/0503077]; S. Baek, P. Hamel, D. London, A. Datta and D. A. Suprun, Phys. Rev. D **71**, 057502 (2005) [arXiv:hep-ph/0412086].
- [8] J. Malcles, arXiv:hep-ph/0606083.
- [9] L. Wolfenstein, Phys. Rev. Lett. **51**, 1945 (1983).
- [10] D. Zeppenfeld, Z. Phys. C **8**, 77 (1981); M. J. Savage and M. B. Wise, Phys. Rev. D **39**, 3346 (1989) [Erratum-ibid. D **40**, 3127 (1989)]; L. L. Chau, H. Y. Cheng, W. K. Sze, H. Yao and B. Tseng, Phys. Rev. D **43**, 2176 (1991) [Erratum-ibid. D **58**, 019902 (1998)]; M. Gronau, O. F. Hernandez, D. London and J. L. Rosner, Phys. Rev. D **50**, 4529 (1994) [hep-ph/9404283]; M. Gronau, O. F. Hernandez, D. London and J. L. Rosner, Phys. Rev. D **52**, 6374 (1995) [hep-ph/9504327].
- [11] S. Eidelman *et al.* [Particle Data Group Collaboration], Phys. Lett. B **592**, 1 (2004) and 2005 partial update for the 2006 edition available on the PDG WWW pages (<http://pdg.lbl.gov/>).
- [12] M. Neubert and J. L. Rosner, Phys. Lett. B **441**, 403 (1998) [hep-ph/9808493]; Phys. Rev. Lett. **81**, 5076 (1998) [hep-ph/9809311]; M. Neubert, JHEP **9902**, 014 (1999) [hep-ph/9812396]; M. Gronau, D. Pirjol and T. M. Yan, Phys. Rev. D **60**, 034021 (1999) [hep-ph/9810482].
- [13] H. n. Li, S. Mishima and A. I. Sanda, Phys. Rev. D **72**, 114005 (2005) [arXiv:hep-ph/0508041].
- [14] Updated results and references are tabulated periodically by the Heavy Flavor Averaging Group:
<http://www.slac.stanford.edu/xorg/hfag/rare>.
- [15] B. Aubert *et al.* [BaBar Collaboration], Phys. Rev. Lett. **94**, 191802 (2005) [arXiv:hep-ex/0502017].
- [16] B. Aubert *et al.* [BaBar Collaboration], Phys. Rev. Lett. **95**, 131803 (2005) [arXiv:hep-ex/0503035].

- [17] B. Aubert *et al.* [BaBar Collaboration], Phys. Rev. D **73**, 071102 (2006) [arXiv:hep-ex/0603013].
- [18] B. Aubert *et al.* [BaBar Collaboration], arXiv:hep-ex/0607063.
- [19] B. Aubert *et al.* [BaBar Collaboration], arXiv:hep-ex/0607096.
- [20] B. Aubert *et al.* [BaBar Collaboration], arXiv:hep-ex/0607106.
- [21] B. Aubert *et al.* [BaBar Collaboration], arXiv:hep-ex/0608003.
- [22] B. Aubert *et al.* [BaBar Collaboration], arXiv:hep-ex/0608036.
- [23] A. Lazzaro, talk presented at XXXIII International Conference on High Energy Physics, Moscow, July 26 - August 2, 2006.
- [24] P. Chang [Belle Collaboration], Phys. Rev. D **71**, 091106 (2005) [arXiv:hep-ex/0412043].
- [25] J. Schümann [Belle Collaboration], Phys. Rev. Lett. **97**, 061802 (2006).
- [26] K. Abe [Belle Collaboration], arXiv:hep-ex/0608033.
- [27] K. Abe [Belle Collaboration], arXiv:hep-ex/0608049.
- [28] K. Abe [Belle Collaboration], arXiv:hep-ex/0609015.
- [29] K. Hara, talk presented at XXXIII International Conference on High Energy Physics, Moscow, July 26 - August 2, 2006.
- [30] S. J. Richichi *et al.* [CLEO Collaboration], Phys. Rev. Lett. **85**, 520 (2000) [hep-ex/9912059].
- [31] D. Cronin-Hennessy *et al.* [CLEO Collaboration], Phys. Rev. Lett. **85**, 515 (2000).
- [32] S. Chen *et al.* [CLEO Collaboration], Phys. Rev. Lett. **85**, 525 (2000) [arXiv:hep-ex/0001009].
- [33] B. H. Behrens *et al.* [CLEO Collaboration], Phys. Rev. Lett. **80**, 3710 (1998) [arXiv:hep-ex/9801012].
- [34] D. M. Asner *et al.* [CLEO Collaboration], Cornell University Report No. CLNS-01/1718, hep-ex/0103040.
- [35] D. Tonelli *et al.* [CDF Collaboration], PoS **HEP2005**, 258 (2006) [arXiv:hep-ex/0512024].
- [36] P. Maksimovic (for the CDF Collaboration), presented at Moriond QCD 2006.
- [37] A. Abulencia *et al.* [CDF Collaboration], arXiv:hep-ex/0607021.

- [38] M. Bona *et al.* [UTfit Collaboration], JHEP **0610**, 081 (2006) [arXiv:hep-ph/0606167].
- [39] X. q. Li and Y. d. Yang, QCD factorization approach,” Phys. Rev. D **72**, 074007 (2005) [arXiv:hep-ph/0508079].
- [40] M. Beneke and S. Jager, Nucl. Phys. B **751**, 160 (2006) [arXiv:hep-ph/0512351].
- [41] M. Beneke, Phys. Lett. B **620**, 143 (2005) [arXiv:hep-ph/0505075].
- [42] C. W. Bauer, I. Z. Rothstein and I. W. Stewart, Phys. Rev. D **74**, 034010 (2006) [arXiv:hep-ph/0510241].
- [43] R. Fleischer and J. Matias, Phys. Rev. D **66**, 054009 (2002) [arXiv:hep-ph/0204101].
- [44] D. London, J. Matias and J. Virto, Phys. Rev. D **71**, 014024 (2005) [arXiv:hep-ph/0410011].
- [45] A. S. Dighe, M. Gronau and J. L. Rosner, Phys. Lett. B **367**, 357 (1996) [hep-ph/9509428]; *Erratum-ibid.* B **377**, 325 (1996); Phys. Rev. Lett. **79**, 4333 (1997) [hep-ph/9707521].
- [46] C. W. Chiang and J. L. Rosner, Phys. Rev. D **65**, 074035 (2002) [Erratum-ibid. D **68**, 039902 (2003)] [arXiv:hep-ph/0112285]; C. W. Chiang, M. Gronau and J. L. Rosner, Phys. Rev. D **68**, 074012 (2003) [hep-ph/0306021].
- [47] H. K. Fu, X. G. He and Y. K. Hsiao, Phys. Rev. D **69**, 074002 (2004) [arXiv:hep-ph/0304242].
- [48] T. Yoshikawa, Phys. Rev. D **68**, 054023 (2003) [arXiv:hep-ph/0306147]; S. Mishima and T. Yoshikawa, Phys. Rev. D **70**, 094024 (2004) [arXiv:hep-ph/0408090].
- [49] A. J. Buras, R. Fleischer, S. Recksiegel and F. Schwab, Eur. Phys. J. C **32**, 45 (2003) [arXiv:hep-ph/0309012]; A. J. Buras, R. Fleischer, S. Recksiegel and F. Schwab, Phys. Rev. Lett. **92**, 101804 (2004) [arXiv:hep-ph/0312259]. Eur. Phys. J. C **45**, 701 (2006) [arXiv:hep-ph/0512032].
- [50] V. Barger, C. W. Chiang, P. Langacker and H. S. Lee, Phys. Lett. B **598**, 218 (2004) [arXiv:hep-ph/0406126].
- [51] S. Baek, JHEP **0607**, 025 (2006) [arXiv:hep-ph/0605094].
- [52] M. Gronau and J. L. Rosner, arXiv:hep-ph/0608040.
- [53] See, for example, the discussions on this issue in M. Imbeault, D. London, C. Sharma, N. Sinha and R. Sinha, arXiv:hep-ph/0608169.
- [54] Y. L. Wu, Y. F. Zhou and C. Zhuang, arXiv:hep-ph/0606035; arXiv:hep-ph/0609006.

Observable	Scheme 1	Scheme 2	Scheme 3	Scheme 4
$Br(\pi^+\pi^-)$	5.3 ± 1.0	5.3 ± 1.0	5.3 ± 1.0	5.3 ± 1.0
$Br(\pi^0\pi^0)$	1.7 ± 0.3	1.7 ± 0.3	1.7 ± 0.3	1.6 ± 0.3
$Br(\pi^-\pi^0)$	4.8 ± 1.0	4.9 ± 1.0	4.9 ± 1.0	5.1 ± 1.1
$Br(\pi^+K^-)$	20.3 ± 1.0	20.2 ± 1.0	20.2 ± 1.0	20.4 ± 4.3
$Br(\pi^0\bar{K}^0)$	9.6 ± 1.0	9.6 ± 0.9	9.6 ± 1.0	9.8 ± 2.3
$Br(\pi^-\bar{K}^0)$	22.6 ± 1.1	22.7 ± 1.1	22.7 ± 1.1	23.1 ± 4.8
$Br(\pi^0K^-)$	12.3 ± 1.2	12.2 ± 1.1	12.3 ± 1.2	12.5 ± 2.7
$Br(K^0\bar{K}^0)$	1.1 ± 0.1	1.1 ± 0.1	1.1 ± 0.1	0.9 ± 0.1
$Br(K^-\bar{K}^0)$	1.2 ± 0.1	1.2 ± 0.1	1.2 ± 0.1	1.0 ± 0.2
$Br(\pi^0\eta)$	1.0 ± 0.1	1.0 ± 0.1	1.0 ± 0.1	0.8 ± 0.1
$Br(\pi^0\eta')$	1.0 ± 0.1	1.0 ± 0.1	1.0 ± 0.1	0.8 ± 0.1
$Br(\pi^-\eta)$	4.6 ± 0.6	4.6 ± 0.6	4.6 ± 0.6	4.6 ± 0.7
$Br(\pi^-\eta')$	3.2 ± 0.3	3.2 ± 0.3	3.2 ± 0.3	3.0 ± 0.4
$Br(\bar{K}^0\eta)$	1.4 ± 0.2	1.3 ± 0.2	1.4 ± 0.2	1.4 ± 0.3
$Br(\bar{K}^0\eta')$	65.3 ± 5.2	65.7 ± 5.0	65.5 ± 4.8	66.4 ± 13.0
$Br(K^-\eta)$	1.5 ± 0.3	1.5 ± 0.2	1.5 ± 0.3	1.5 ± 0.4
$Br(K^-\eta')$	69.2 ± 5.5	69.5 ± 5.3	69.3 ± 5.1	70.1 ± 13.8
$Br(\eta\eta)$	0.8 ± 0.1	0.8 ± 0.1	0.8 ± 0.1	0.8 ± 0.1
$Br(\eta'\eta')$	0.4 ± 0.0	0.4 ± 0.0	0.4 ± 0.0	0.4 ± 0.0
$Br(\eta\eta')$	1.2 ± 0.1	1.2 ± 0.1	1.2 ± 0.1	1.1 ± 0.1
$\mathcal{A}(\pi^+\pi^-)$	0.27 ± 0.06	0.24 ± 0.05	0.25 ± 0.05	0.22 ± 0.04
$\mathcal{A}(\pi^0\pi^0)$	0.71 ± 0.10	0.70 ± 0.10	0.70 ± 0.10	0.67 ± 0.09
$A_{CP}(\pi^-\pi^0)$	0.03 ± 0.03	0.02 ± 0.03	0.03 ± 0.03	0.04 ± 0.03
$A_{CP}(\pi^+K^-)$	-0.07 ± 0.02	-0.08 ± 0.02	-0.08 ± 0.02	-0.08 ± 0.02
$\mathcal{A}(\pi^0K_S)$	-0.13 ± 0.02	-0.12 ± 0.02	-0.15 ± 0.03	-0.17 ± 0.03
$A_{CP}(\pi^-\eta)$	-0.09 ± 0.10	-0.11 ± 0.09	-0.10 ± 0.09	-0.10 ± 0.09
$A_{CP}(\pi^-\eta')$	0.06 ± 0.12	0.04 ± 0.12	0.04 ± 0.12	0.02 ± 0.11
$\mathcal{A}(\eta K_S)$	0.13 ± 0.07	0.14 ± 0.07	0.16 ± 0.08	0.18 ± 0.09
$\mathcal{A}(\eta' K_S)$	0.02 ± 0.00	0.02 ± 0.00	0.03 ± 0.01	0.03 ± 0.01
$A_{CP}(K^-\eta)$	-0.25 ± 0.12	-0.29 ± 0.13	-0.27 ± 0.14	-0.29 ± 0.15
$\mathcal{A}(\eta\eta)$	-0.77 ± 0.11	-0.78 ± 0.11	-0.76 ± 0.11	-0.73 ± 0.11
$\mathcal{A}(\eta'\eta')$	-0.55 ± 0.13	-0.55 ± 0.13	-0.55 ± 0.13	-0.58 ± 0.13
$\mathcal{A}(\eta\eta')$	-0.65 ± 0.13	-0.66 ± 0.13	-0.66 ± 0.12	-0.66 ± 0.12
$\mathcal{S}(\pi^+\pi^-)$	-0.533 ± 0.135	-0.533 ± 0.135	-0.532 ± 0.134	-0.513 ± 0.138
$\mathcal{S}(\pi^0\pi^0)$	0.634 ± 0.116	0.655 ± 0.111	0.649 ± 0.111	0.614 ± 0.118
$\mathcal{S}(\pi^0K_S)$	0.780 ± 0.041	0.781 ± 0.041	0.789 ± 0.041	0.791 ± 0.041
$\mathcal{S}(K^0\bar{K}^0)$	-0.001 ± 0.031	-0.001 ± 0.031	-0.001 ± 0.030	-0.000 ± 0.017
$\mathcal{S}(\eta K_S)$	0.5 ± 0.06	0.5 ± 0.05	0.45 ± 0.06	0.39 ± 0.07
$\mathcal{S}(\eta' K_S)$	0.72 ± 0.04	0.72 ± 0.04	0.72 ± 0.04	0.71 ± 0.04

Table 7: Predicted branching ratios (in units of 10^{-6}) and CP asymmetries for all the PP modes of $B^{0,+}$ decays in different schemes. Vanishing observables in our approach are omitted.

Observable	Scheme 1	Scheme 2	Scheme 3	Scheme 4
$Br(\pi^+\pi^-)$	0	0	0	0
$Br(\pi^0\pi^0)$	0	0	0	0
$Br(\pi^+K^-)$	5.0 ± 0.9	5.0 ± 0.9	5.0 ± 0.9	5.0 ± 0.9
$Br(\pi^0K^0)$	1.6 ± 0.3	1.6 ± 0.3	1.6 ± 0.3	1.5 ± 0.3
$Br(K^+K^-)$	18.9 ± 1.0	18.9 ± 1.0	18.9 ± 1.0	19.1 ± 4.0
$Br(K^0K^0)$	19.7 ± 1.0	19.8 ± 1.0	19.8 ± 1.0	20.2 ± 4.2
$Br(\pi^0\eta)$	0	0	0.1 ± 0.0	0.1 ± 0.0
$Br(\pi^0\eta')$	0.1 ± 0.0	0.1 ± 0.0	0.1 ± 0.0	0.1 ± 0.1
$Br(\bar{K}^0\eta)$	0.7 ± 0.2	0.7 ± 0.2	0.7 ± 0.2	0.7 ± 0.2
$Br(\bar{K}^0\eta')$	3.3 ± 0.3	3.4 ± 0.3	3.4 ± 0.3	2.8 ± 0.3
$Br(\eta\eta)$	2.0 ± 0.4	2.0 ± 0.4	2.0 ± 0.4	2.0 ± 0.6
$Br(\eta'\eta')$	48.3 ± 4.4	48.6 ± 4.3	48.3 ± 4.1	48.9 ± 9.8
$Br(\eta\eta')$	22.4 ± 1.5	22.6 ± 1.4	22.5 ± 1.4	22.9 ± 4.7
$\mathcal{A}(\pi^+\pi^-)$	0	0	0	0
$\mathcal{A}(\pi^0\pi^0)$	0	0	0	0
$A_{CP}(\pi^+K^-)$	0.27 ± 0.06	0.24 ± 0.05	0.25 ± 0.05	0.22 ± 0.04
$\mathcal{A}(\pi^0K_S)$	0.71 ± 0.10	0.70 ± 0.10	0.70 ± 0.10	0.67 ± 0.09
$\mathcal{A}(K^+K^-)$	-0.07 ± 0.02	-0.08 ± 0.02	-0.08 ± 0.02	-0.08 ± 0.02
$\mathcal{A}(K^0K^0)$	0	0	0	0
$\mathcal{A}(\pi^0\eta)$	0.20 ± 0.47	0.32 ± 0.48	0.19 ± 0.46	0.18 ± 0.45
$\mathcal{A}(\pi^0\eta')$	0.20 ± 0.47	0.32 ± 0.48	0.19 ± 0.46	0.18 ± 0.45
$\mathcal{A}(\eta K_S)$	-0.24 ± 0.13	-0.27 ± 0.13	-0.26 ± 0.12	-0.22 ± 0.11
$\mathcal{A}(\eta' K_S)$	-0.42 ± 0.08	-0.41 ± 0.08	-0.41 ± 0.08	-0.45 ± 0.08
$\mathcal{A}(\eta\eta)$	-0.20 ± 0.03	-0.20 ± 0.03	-0.24 ± 0.04	-0.27 ± 0.05
$\mathcal{A}(\eta'\eta')$	0.03 ± 0.01	0.03 ± 0.01	0.03 ± 0.01	0.04 ± 0.01
$\mathcal{A}(\eta\eta')$	-0.02 ± 0.00	-0.02 ± 0.00	-0.03 ± 0.01	-0.03 ± 0.01
$\mathcal{S}(\pi^+\pi^-)$	0	0	0	0
$\mathcal{S}(\pi^0\pi^0)$	0	0	0	0
$\mathcal{S}(\pi^0K_S)$	0.282 ± 0.158	0.318 ± 0.153	0.311 ± 0.153	0.185 ± 0.167
$\mathcal{S}(K^+K^-)$	0.167 ± 0.024	0.217 ± 0.030	0.216 ± 0.030	0.244 ± 0.037
$\mathcal{S}(K^0K^0)$	-0.041 ± 0.004	-0.041 ± 0.004	-0.041 ± 0.004	-0.040 ± 0.003
$\mathcal{S}(\eta K_S)$	0.26 ± 0.17	0.24 ± 0.17	0.26 ± 0.17	0.26 ± 0.16
$\mathcal{S}(\eta' K_S)$	0.40 ± 0.08	0.39 ± 0.08	0.39 ± 0.08	0.45 ± 0.08

Table 8: Predicted branching ratios (in units of 10^{-6}) and CP asymmetries for all the PP modes of B_s decays in different schemes. Observables with vanishing entries are omitted.